Clinical Chemistry 45:9
1621–1627 (1999)

Oak Ridge Conference

Evaluation of Measurement Sites for Noninvasive Blood Glucose Sensing with Near-Infrared Transmission Spectroscopy

Jason J. Burmeister* and Mark A. Arnold†

Six putative measurement sites were evaluated for noninvasive sensing of blood glucose by first-overtone near-infrared spectroscopy. The cheek, lower lip, upper lip, nasal septum, tongue, and webbing tissue between the thumb and forefinger were examined. These sites were evaluated on the basis of their chemical and physical properties as they pertain to the noninvasive measurement of glucose. Critical features included the effective optical pathlength of aqueous material within the tissue and the percentage of body fat within the optical path. Aqueous optical paths of 5 mm are required to measure clinically relevant concentrations of glucose in the first-overtone region. All of the tested sites met this requirement. The percentage of body fat affects the signal-to-noise ratio of the measurement and must be minimized for reliable glucose sensing. The webbing tissue contains a considerable amount of fat tissue and is clearly the worse measurement site. All other sites possess substantially less fat, with the least amount of fat in tongue tissue. For this reason, the tongue provides spectra with the highest signal-to-noise ratio and is, therefore, the site of choice on the basis of spectral quality.

Measurement site is a critical factor for noninvasive spectroscopic blood glucose sensing in human subjects. The index finger *(1, 2)*, the inner portion of the lower lip *(3–5)*, the forearm *(6)*, and the webbing tissue between the thumb and forefinger *(7)* have been proposed for noninvasive measurements with near-infrared (near-IR)[1] spectroscopy. Ocular measurements have also been suggested but mainly with Raman spectroscopy and optical rotation *(8–10)*. Regardless of the optical technique, the chemical and physical properties of the measurement site are critical because they influence, and may possibly dictate, the overall signal-to-noise ratio (SNR) of the measurement.

Scattering and molecular absorption combine to attenuate near-IR light as it passes through human tissue. The principal phenomena responsible for light attenuation depend on the spectral range. Molecular absorption dominates in the combination spectral range (2.0–2.5 μm) where water, fat, and protein are the primary absorbers. In comparison, scattering is more important in the first-overtone region (1.52–1.85 μm), although molecular absorption by water and fat is still significant. The impact of protein is much less in the first-overtone region compared with the combination region *(11)*. The thickness of the tissue within the measurement site is critical regardless of the spectral range. The tissue must be thick enough to provide sufficient glucose for reliable detection and yet thin enough to yield sufficiently large radiant powers for high spectral quality. The composition and thickness of the tissue probed by the transmitting radiation strongly impact analytical performance by affecting the SNR of the measurement.

In this study, first-overtone near-IR spectra collected noninvasively from human subjects are characterized with the goal of identifying potential measurement sites for research purposes. Results from an in vitro model *(11)* are used to identify the chemical and physical properties of the ideal measurement site. Noninvasive human spectra are presented for several potential measurement sites. The amounts of water and fat within the probed tissue are estimated by a regression analysis. The suitability of each

Department of Chemistry and Optical Science and Technology Center, University of Iowa, Iowa City, IA 52242.

*Present address: Departments of Psychiatry and Pharmacology and Rocky Mountain Center for Sensor Technology, University of Colorado Health Sciences Center, Denver, CO 80262.

†Author for correspondence. Fax 319-353-1115; e-mail mark-arnold@uiowa.edu.

Received May 7, 1999; accepted July 1, 1999.

[1] Nonstandard abbreviations: Near-IR, near-infrared; SNR, signal-to-noise ratio; InGaAs, indium-gallium-arsenide; RMSN-100%, root-mean-square noise on 100% lines; and μAU, microabsorbance unit(s).

putative measurement site is evaluated on the basis of the effective aqueous pathlength and the amount of fatty tissue. Results identify the tongue as an excellent measurement site for noninvasive human spectra over the first-overtone region.

Materials and Methods

INSTRUMENTATION

Near-IR spectra for the in vitro model were collected with a modified Nicolet 740 Fourier transform infrared spectrometer. This spectrometer was equipped with a 400 W tungsten-halogen lamp, calcium fluoride beam splitter, and a 1-mm indium-gallium-arsenide (InGaAs) detector (ETX-1000T-GR1.9; Eppitax) operating at room temperature.

Noninvasive human spectra were collected with a modified Midac M series Fourier transform infrared spectrometer. Details of these modifications are provided elsewhere *(12)*. Briefly, the original source was replaced with a 150 W tungsten-halogen lamp configured as a projector bulb with a back-reflector plate (model EFR; Apollo). This lamp was powered by a DCR 40-13B2 DC power supply from Sorensen. A 630 nm interference filter was positioned in front of each photodiode detector associated with the interferometer. These filters were necessary to prevent detector saturation by the strong incident radiation of the 150 W source. The internal temperature of the interferometer housing was controlled by a feedback air-cooling system. The internal temperature of the interferometer housing was measured and used to control the speed of the cooling fan. This arrangement permitted operation at 41.0 °C with constant control to ± 0.1 °C. The mirror velocity was set at 0.24 cm/s, which represented the most stable mirror movement of the available settings. Finally, a 1-mm diameter, thermally electric cooled, InGaAs detector (ETX-1000TE-GR1.9; Eppitax) was incorporated into the spectrometer. The detector temperature was maintained at 15 °C to lower the noise relative to room temperature and still provide high detectivity up to 1.82 μm.

REAGENTS

Aqueous solutions were prepared in 0.1 mol/L phosphate buffer maintained at pH 7.35 with 4.4 g/L 5-fluorouracil added to prevent bacterial contamination. Glucose solutions were prepared by dissolving weighed, dried amounts of reagent-grade material. Fat tissue was from bovine samples obtained from a local supermarket. Fat filters were prepared as described previously *(11)* by sandwiching a known amount of blended fat material between parallel sapphire windows with Teflon spacers. Bundles of quartz fibers were purchased from Dolan Jenner Industries.

PROCEDURES

In vitro models of the human body were prepared as described previously *(11)* by combining individual layers of fatty tissue and aqueous buffer. The relative thickness of each layer was adjusted so that the first-overtone spectra collected from the in vitro model closely matched those obtained from a given measurement site on a particular subject *(11)*.

In vivo spectra were collected either by using a fiber optic probe or by focusing the incident beam directly onto the tissue section of interest. In both cases, the tissue section in question was sandwiched between two flat sapphire windows. In the fiber optic configuration, one fiber bundle was used to bring the incident light from the source optics to the measurement site. A fraction of the transmitted radiation was collected by a second fiber bundle, and this light was directed to the detection optics. This fiber optic arrangement permitted collection of spectra from hard to reach locations. Considerable losses of radiant power through the fiber-optic couplings, however, led to low SNRs and poor spectral quality. Higher SNRs were achieved by directly focusing the incident radiation onto the tissue. A 1-inch diameter, 25-mm focal length convex lens was used to focus the incident beam onto the sample tissue. The InGaAs detector module was positioned immediately behind the tissue with the window on the photodiode casing touching the sapphire window. The best performance was obtained by focusing the incident light through the sample tissue onto the surface of the photodiode.

In vivo absorbance spectra were computed from single-beam tissue spectra and attenuated single-beam air background spectra. Single-beam air background spectra were collected in either the fiber optic or direct focusing configuration described above. Neutral density filters with known percentages of transmissions were used to attenuate the air spectra and avoid detector saturation. Intensity values for each air background spectrum were multiplied by the appropriate factor to account for the extent of attenuation provided by the neutral density filter. Similarly, each background spectrum was adjusted to account for any differences in instrument gain settings between a given air background and the corresponding sample spectrum. Absolute absorbance was then estimated using the ratio of each sample spectrum to the corresponding "corrected" air background spectrum.

Effective optical pathlengths through the fat and aqueous regions of the tested measurement sites were estimated by the regression method described in detail elsewhere *(11)*. Briefly, the tissue of interest was sandwiched between two sapphire windows, and calipers were used to measure the combined thickness of the tissue/window assembly. The thickness of the tissue section was calculated by subtracting the known window thickness. Absolute absorbance spectra collected noninvasively from human tissue were fitted by regression to standard absorbance spectra for fat and water. The regression calculation was performed according to the following expression:

$$S_T = \beta_0 + \beta_1 S_w + \beta_2 S_f \quad (1)$$

where S_T, S_w, and S_f correspond to absolute absorbance spectra for known thickness of tissue, water, and fat, respectively, and β_i values represent the corresponding regression coefficients. Effective optical pathlengths were obtained by multiplying the respective regression coefficients by the known thicknesses of the individual standard materials of fat and water.

Results and Discussion

Noninvasive blood glucose sensing by near-IR spectroscopy requires glucose-dependent absorption of near-IR light as it passes through a selected region of the human body. Clearly, the amount of light absorbed by glucose must be significantly greater than intensity fluctuations caused by measurement noise. Both sensitivity and accuracy demand high SNRs, where high signals correspond to large absorbance values originating from glucose and low noise corresponds to performance of the instrumentation. Selection of a measurement site must consider the physical and chemical characteristics as they pertain to the overall SNR.

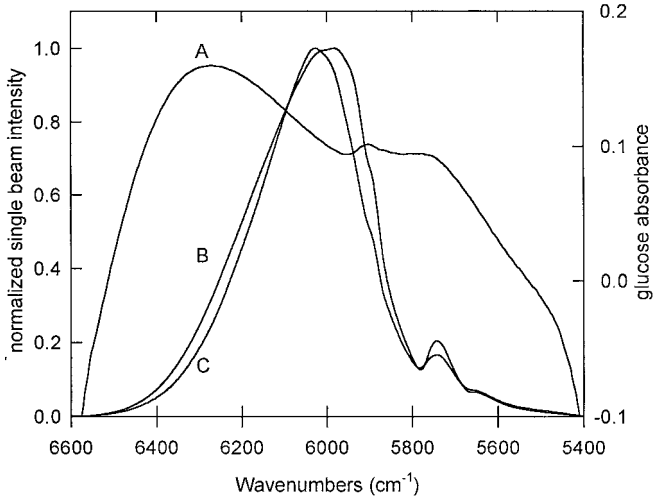

Fig. 1. First-overtone absorbance spectrum of a 1 mol/L aqueous glucose solution (*spectrum A*), a single-beam spectrum collected through the in vitro model of human tissue (*spectrum B*), and a corresponding noninvasive single-beam spectrum collected through human webbing tissue (*spectrum C*).

PHYSICAL AND CHEMICAL REQUIREMENTS

The Beer-Lambert law of absorption spectroscopy indicates that glucose absorbance values depend on the absorptivity, concentration, and optical pathlength. Molar absorptivity is fixed at each wavelength by the vibrational absorption properties of glucose. The concentration range is defined by the intended clinical application and is generally 2–22 mmol/L (36–396 mg/dL) for blood glucose. Optical pathlength is the only adjustable experimental parameter, which makes it vitally important when designing noninvasive measurement technology. The optical pathlength must be sufficiently long to allow enough glucose molecules within the optical path to produce a measurable absorbance signal. If the optical pathlength is too long, however, excessive light attenuation will increase noise by reducing radiant power at the detector. The ideal pathlength depends on instrumental performance and spectral range.

Instrumental performance is best represented as the root-mean-square noise on 100% lines (RMSN-100%). This value is obtained by collecting two single-beam spectra for the exact same sample. One spectrum is divided by the other, and in the ideal case of no noise or spectrometer variation, the result is a horizontal line at 1.00 (or 100% transmission). Both spectrometer noise and instrument variation are clearly evident when the resulting product ratio is plotted as a function of wavelength [see Fig. 2 in Ref. *(13)*]. As is detailed elsewhere, the RMSN-100% tracks the optical throughput of the sample with lower noise at higher throughput *(13, 14)*. It is convenient to report the RMSN-100% in microabsorbance units (μAU) by converting the percentage of transmission to absorbance units [log (1/T)]. The actual RMSN-100% value is found by fitting the data to either a first- or second-order polynomial function and computing the root-mean-square value for the data relative to this fitted function. RMSN-100% values are best provided over a series of defined and narrow spectral regions. Generally, values computed over wide spectral ranges will be dominated by the noisiest regions, making it difficult to characterize spectral quality in the lower-noise regions where most of the analyte-specific information resides.

Spectral range is critical because the shape and size of the glucose absorption features differ significantly in the combination *(15–17)*, first-overtone *(14)*, and short-wavelength *(17, 18)* regions of the near-IR spectrum. The focus of this report is the first-overtone region, where optical pathlengths of 5–10 mm are necessary to measure clinically relevant concentrations of glucose in aqueous solutions *(14)*. Our previous work indicated that prediction errors <0.6 mmol/L are possible for glucose but only with 5–10 mm optical pathlengths coupled with RMSN-100% values <10 μAU over the 5975–5850 cm^{-1} spectral range *(14)*. These values were established under ideal conditions with a Fourier transform spectrometer in combination with fixed optical pathlengths and controlled sample temperatures.

FEATURES OF NONINVASIVE HUMAN SPECTRA

Absorbance spectra collected across human tissue are dominated by the absorption properties of water and fatty tissue *(11)*. The high water content of body tissue and the high absorptivity of O—H absorption bands at 7000 and 5200 cm^{-1} restrict the optical transmission window for first-overtone spectra to 6400–5600 cm^{-1}. First overtones of C—H vibrations are located within this optical window. The high CH content of body fat is evident within in vivo spectra, in which fat absorption is observed as two strong, overlapping absorbance bands centered at 5790

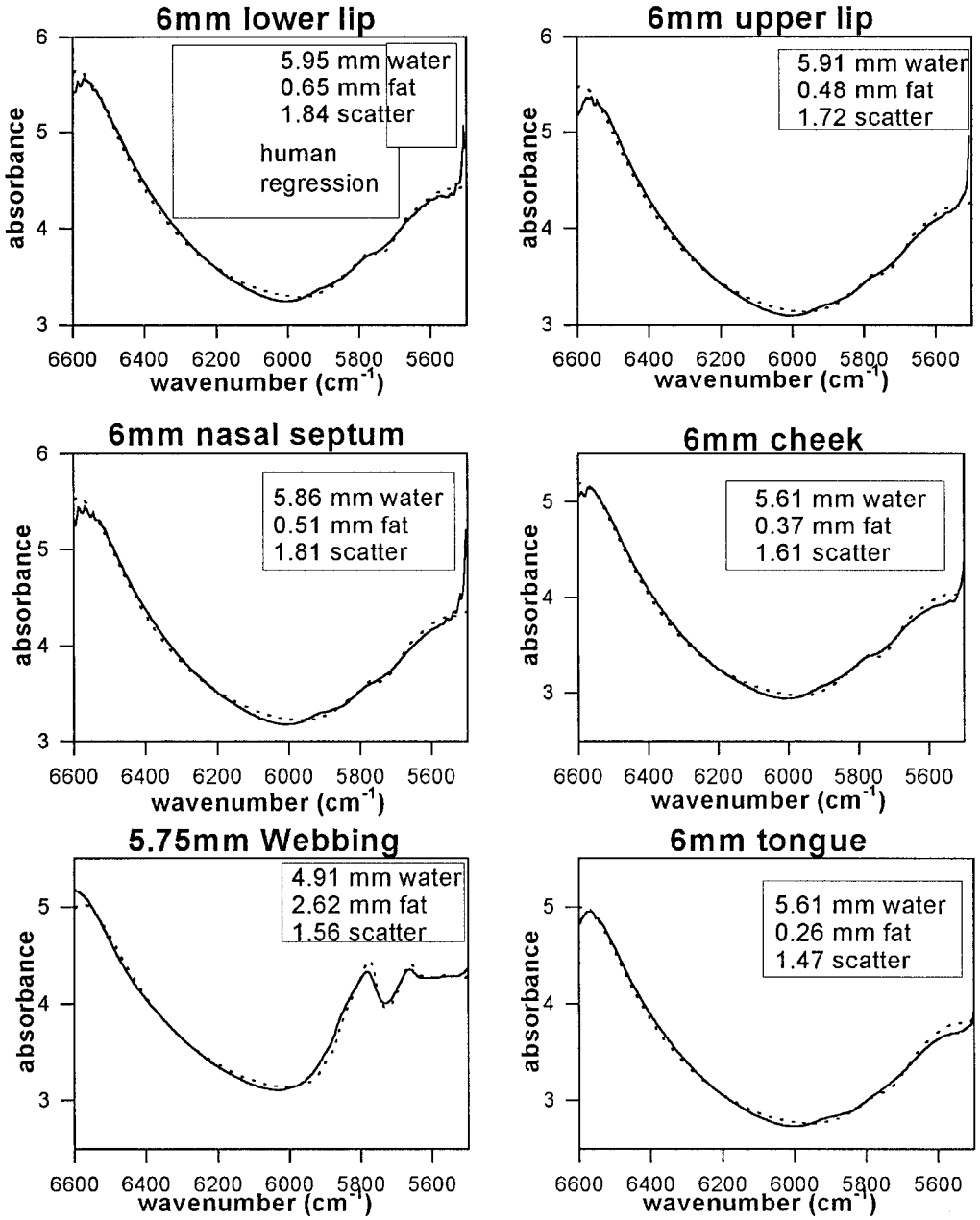

Fig. 2. Absorbance spectra for the indicated measurement sites (*solid lines*) and fitted spectra based on Eq. 1 (*dashed lines*).

and 5690 cm^{-1}. Glucose, on the other hand, possesses three absorption bands centered at 6200, 5920, and 5775 cm^{-1}. Fundamental studies indicate the optimum region for partial least-squares modeling is the 5975–5850 cm^{-1} spectral range, which includes the 5920 cm^{-1} absorption band of glucose *(14)*.

The first-overtone spectrum in Fig. 1 illustrates the effective transmission window through human tissue. Fig. 1 includes a single-beam spectrum collected across the webbing tissue between the thumb and forefinger (spectrum C), a single-beam spectrum of a matching in vitro model (spectrum B), and an absorbance spectrum of dissolved glucose (spectrum A). Comparison of these spectra reveals the principal complication caused by body fat when attempting to measure glucose from noninvasive human spectra. Fatty tissue absorbs significant amounts of the incident radiation over an important portion of the glucose absorbance spectrum. Fat absorption reduces the optical throughput over the critical 5920 cm^{-1} glucose absorption band, thereby adversely affecting spectral quality by reducing the SNR for the measurement. This point is clear when comparing RMSN-100% values for webbing and buffer spectra. A typical RMSN-100% value over the 6000–5900 cm^{-1} spectral range is 271.1 μAU for a 6.0-mm thick sample of webbing tissue (see Table 2 below). Over this same spectral range, RMSN-100% val-

Table 1. Tissue thickness and optical paths for putative measurement sites.

	Webbing	Tongue	Upper lip	Lower lip	Nasal septum	Cheek
Tissue thickness, mm	5.75	6.00	6.00	6.00	6.00	6.00
Effective optical pathlengths through water, mm	4.91	5.61	5.91	5.95	5.86	5.61
Effective optical pathlengths through fat, mm	2.62	0.26	0.48	0.65	0.51	0.37

ues are ~5–9 μAU for water samples with similar thickness (5.2 and 10 mm) *(14)*. Fat within the webbing reduces spectral quality by a factor of 30–50 right in the most important spectral region for glucose.

The impact of body fat on the ability to measure glucose from spectra collected noninvasively from the human body stems from a reduction in optical throughput over the spectral range that contains glucose-specific information. Fortunately, the absorption features of glucose do not overlap directly with those of fatty tissue but are shifted slightly to higher frequencies.

PUTATIVE MEASUREMENT SITES

From the above analysis, the ideal measurement site for noninvasive first-overtone spectra provides an effective aqueous pathlength of 5–10 mm, high radiant throughput, and minimal body fat. Various putative measurement sites were evaluated to identify those that most closely match these characteristics. Spectra from the tongue, nasal septum, cheek, upper lip, lower lip, and the webbing tissue between the thumb and forefinger were examined.

Sample absorbance spectra are presented in Fig. 2 for the examined tissues. Each spectrum in Fig. 2 includes the measured absorbance spectrum (relative to an air background) along with the fitted spectrum from the regression analysis based on Eq. 1. These spectral results correspond to 6-mm thick samples of tissue for all sites except the webbing, which corresponds to a thickness of 5.75 mm. The fat absorption bands are evident in the webbing spectrum. Conversely, the magnitude of fat absorption is strikingly lower for the other five measurement sites.

Regression analysis can be used to estimate the amounts of fat and water in the optical path. Results of this regression analysis are presented in Table 1 for the various tested measurement sites. These values corroborate inspection of the absorbance spectra and indicate that the amount of fat tissue is substantially less in all tested tissues relative to the webbing. The tongue possesses the lowest fat content overall, with a fat thickness one order of magnitude lower than the webbing.

COMPARISON BETWEEN WEBBING AND TONGUE TISSUES

Individual webbing spectra were collected from 19 volunteers. In each case, the webbing tissue was held snugly between two sapphire windows maintained 5.75 mm apart. The regression analysis indicates the effective optical pathlength through water and fat regions of the tissue. The effective optical pathlengths for the webbing were 4.67 ± 0.41 mm through water and 2.4 ± 0.52 mm through fat. Similarly, tongue spectra were collected from 10 volunteers. In this case, the distance between the sapphire windows was 6 mm, and the regression analysis revealed effective optical pathlengths through water and fat of 5.90 ± 0.30 mm and 0.20 ± 0.04 mm, respectively. These values are consistent with those found in our screening experiment and reported in Table 1.

Differences in optical throughput across webbing and tongue tissues are evident in Fig. 3. The single-beam spectra presented in Fig. 3 were collected under identical instrumental conditions for 6-mm thick samples of webbing and tongue tissues. An absorbance spectrum of glucose is also provided to enhance the comparison. Clearly, the tongue spectrum offers greater radiant throughput, particularly in the region of the 5920 cm^{-1} glucose absorption band. The larger radiant powers at the detector should provide high spectral quality for the tongue spectra.

Spectral quality can be judged by comparing RMSN-100% values computed for these two tissues. In this analysis, 10 back-to-back single beam spectra were collected for each tissue type. Samples were removed and reinserted into the sample holder between each spectrum. The RMSN-100% values were then computed for sequentially collected spectra. The mean values for each tissue are tabulated in Table 2 for 100 cm^{-1} segments over the 6400–5800 cm^{-1} spectral range. The magnitude of these

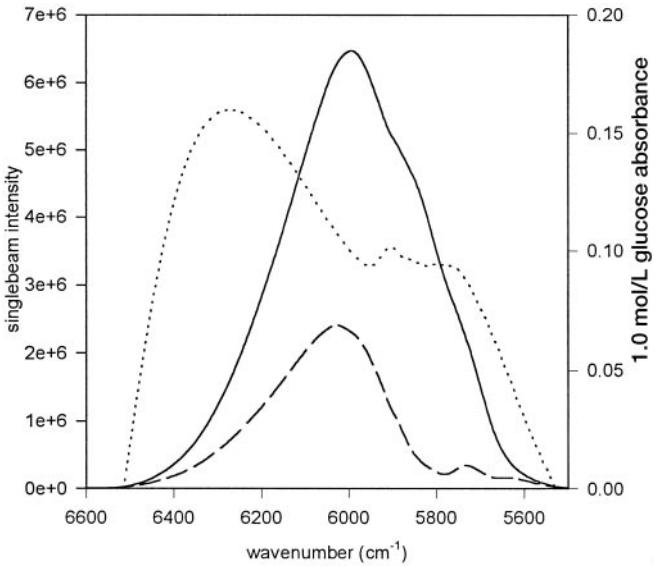

Fig. 3. Noninvasive single-beam spectra for tongue (——) and webbing tissue (– – – –) collected under identical instrumental conditions, and representative glucose absorbance spectrum (· · · · · ·).

Table 2. RMSN-100% values[a] for repetitive tongue and webbing spectra.

Sample	6400–6300[b]	6300–6200[b]	6200–6100[b]	6100–6000[b]	6000–5900[b]	5900–5800[b]
6-mm webbing	54.7	25.1	18.0	36.1	271.1	605.8
5.5-mm tongue	96.7	47.7	25.4	18.0	56.6	68.1

[a] RMSN-100% values computed with second-order polynomial fits and reported in μAU.

[b] Wavenumber range, in cm^{-1}.

RMSN-100% values reflect both the optical throughput of the measurement and the reproducibility of sampling the tissue between sequential spectra.

The RMSN-100% values were lower for the tongue tissue over the spectral ranges lower than 6100 cm^{-1}. The differences are most striking between 6000–5900 and 5900–5800 cm^{-1} where fat absorbs. Fig. 4 shows representative 100% lines obtained from this experiment. Systematic variations in the 100% lines for webbing tissue correspond to absorption bands for fatty tissue. The presence of such features in these 100% lines illustrates the variability induced by sampling slightly different regions of the tissue in question. The superimposed glucose absorbance spectrum highlights the impact of this fat-induced variance on the glucose measurement. In contrast, the representative 100% lines for the tongue spectra show very little variation in the fat-sensitive spectral region. The lower RMSN-100% values reflect this reduction in variance.

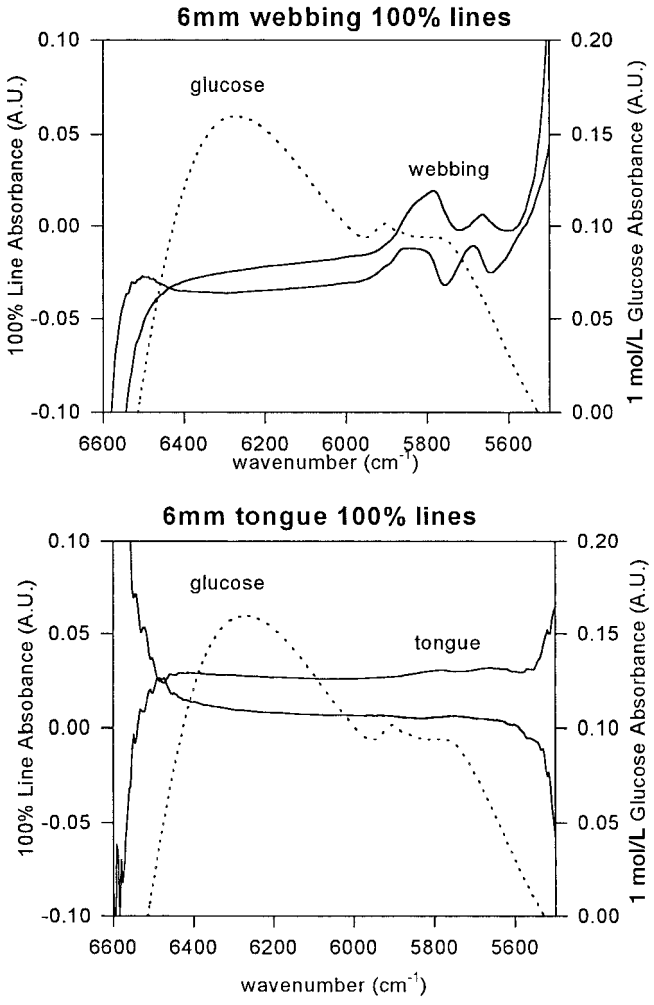

Fig. 4. Sample 100% lines (*solid lines*) for 6-mm thick sample of webbing tissue (*top*) and 6-mm thick sample of tongue (*bottom*) along with representative glucose absorbance spectrum (*dashed lines*).

The RMSN-100% values reported in Table 2 for the spectral regions above 6100 cm^{-1} reveal poorer spectral quality for the tongue tissue relative to the webbing. These results reflect a challenge when working with the tongue as a measurement site. The challenge is to stabilize the tongue while the spectrum is being recorded. Each spectrum requires 1 min for collection. With the sample holder used in this experiment, the tongue must be fully extended throughout this entire period. Slight movements during data collection are unavoidable and certainly add variation to the measurement. Conversely, the webbing tissue is easier to hold in a constant position during data collection. Higher RMSN-100% values for the tongue spectra reflect this difference between these two measurement sites.

Conclusions

The chemical and physical properties of the tongue make it an excellent site for noninvasive glucose measurements with first-overtone near-IR spectroscopy. Transmission through the tongue produces effective optical pathlengths through water of >5 mm, which are required for measuring clinically relevant concentrations of glucose. Furthermore, tongue tissue contains little fat, which permits low noise in the spectral region where the most reliable glucose-specific information resides. Comparing the putative sites examined here, webbing tissue contains the largest percentage of fatty tissue and, therefore, is clearly the worst measurement site. Differences in the amount of fat are considerably less between the remaining measurement sites. Overall, the order of fat content (from highest to lowest) is webbing $\gg$ lower lip > upper lip > cheek > tongue.

This work was supported in part by a grant from the National Institute of Diabetes and Digestive and Kidney Diseases (DK-46126). Portions of this work were supported by a grant from Selfcare, Inc.

References

1. Jagemann K, Fischbacher C, Danzer K, Müller UA, Mertes B. Application of near-infrared spectroscopy for non-invasive determination of blood/tissue glucose using neural networks. Z Phys Chem 1995;191:179–90.
2. Robinson MR, Eaton RP, Haaland DM, Koepp GW, Thomas EV, Stallard BR, Robinson RL. Noninvasive glucose monitoring in

diabetic patients: a preliminary evaluation. Clin Chem 1992;38: 1618–22.

3. Heise HM, Marbach R, Koschinsky TH, Gries FA. Noninvasive blood glucose sensors based on near-infrared spectroscopy. Artif Organs 1994;18:439–47.
4. Marbach R, Koschinsky TH, Gries FA, Heise HM. Noninvasive blood glucose assay by near-infrared diffuse reflectance spectroscopy of the human inner lip. Appl Spectrosc 1993;47:875–81.
5. Heise HM. Non-invasive monitoring of metabolites using near infrared spectroscopy: state of the art. Horm Metab Res 1996; 28:527–34.
6. Malin SF, Ruchti TL, Blank TB, Thennadil SN, Monfre SL. The noninvasive measurement of glucose by near-infrared diffuse reflectance spectroscopy. Clin Chem 1999;45:1651–8.
7. Hazen KH. Glucose determination in biological matrices using near-infrared spectroscopy [PhD Dissertation]. Iowa City, IA: University of Iowa, 1995:315 pp.
8. Cameron BD, Gorde HW, Satheesan B, Coté GL. The use of polarized laser light through the eye for noninvasive glucose monitoring. Diabetes Technol Ther 1999;in press.
9. Steffes PG. Laser-based measurement of glucose in the ocular aqueous humor: An efficacious portal for determination of serum glucose levels. Diabetes Technol Ther 1999;1:129–33.
10. Borchert MS, Storrie-Lombardi MC, Lambert JL. A non-invasive glucose monitor: preliminary results in rabbits. Diabetes Technol Ther 1999;1:145–51.
11. Burmeister JJ, Chung H, Arnold MA. Phantoms for noninvasive blood glucose sensing with near infrared transmission spectroscopy. Photochem Photobiol 1998;67:50–5.
12. Burmeister JJ. In vitro model for human noninvasive blood glucose measurements [PhD Dissertation]. Iowa City, IA: University of Iowa, 1997:170 pp.
13. Hazen KH, Arnold MA, Small GW. Measurement of glucose and other analytes in undiluted human serum with near-infrared transmission spectroscopy. Anal Chim Acta 1998;371:255–67.
14. Hazen KH, Arnold MA, Small GW. Measurement of glucose in water with first-overtone near-infrared spectra. Appl Spectrosc 1998;52:1597–605.
15. Marquardt LA, Arnold MA, Small GW. Near infrared spectroscopic measurement of glucose in a protein matrix. Anal Chem 1993; 65:3271–8.
16. Chung H, Arnold MA, Rhiel M, Murhammer DW. Simultaneous measurements of glucose, glutamine, ammonia, lactate and glutamate in aqueous solutions by near-infrared spectroscopy. Appl Spectrosc 1996;50:270–6.
17. Khalil OS. Spectroscopic and clinical aspects of noninvasive glucose measurements. Clin Chem 1999;45:165–77.
18. Kohl M, Essenpreis M, Cope M. The influence of glucose concentration upon the transport of light in tissue-simulation phantoms. Phys Med Biol 1995;40:1267–87.